NACA TN 2219

NATIONAL ADVISORY COMMITTEE FOR AERONAUTICS

TECHNICAL NOTE 2219

THE DYNAMIC LATERAL CONTROL CHARACTERISTICS OF AIRPLANE MODELS HAVING UNSWEPT WINGS WITH ROUND- AND SHARP-LEADING-EDGE SECTIONS

By James L. Hassell and Charles V. Bennett

Langley Aeronautical Laboratory
Langley Air Force Base, Va.

NACA

Washington
November 1950

NATIONAL ADVISORY COMMITTEE FOR AERONAUTICS

TECHNICAL NOTE 2219

THE DYNAMIC LATERAL CONTROL CHARACTERISTICS OF AIRPLANE MODELS HAVING UNSWEPT WINGS WITH ROUND- AND SHARP-LEADING-EDGE SECTIONS

By James L. Hassell and Charles V. Bennett

SUMMARY

An investigation has been conducted in the Langley free-flight tunnel for the purpose of comparing the dynamic lateral control characteristics of airplane models with round- and sharp-leading-edge wing sections. The two dynamic models used in the investigation had different mass characteristics. One model was representative of a present-day fighter airplane with respect to inertia; the other was representative of a possible future type having very high fuselage inertia. These models could be equipped with either a 12-percent-thick biconvex section wing or an NACA 0012 wing having the same unswept plan forms. The investigation consisted of static and rotary force tests made for the purpose of establishing flight conditions, and flight tests from which the dynamic lateral control characteristics of the models with the two wings were evaluated.

For the flight conditions investigated no apparent effect of airfoil section on the flying characteristics of the model having high inertia in yaw was noted, even for low values of directional stability. The normal-inertia model equipped with the NACA 0012 wing showed an adverse yawing motion in aileron rolls which increased with reduced values of directional stability; when this model was equipped with the 12-percent-thick biconvex wing, however, almost no yawing occurred, even at the lowest values of directional stability. The difference in the yawing characteristics of the models with the two wings was attributed to the effect of C_{n_p}, the rate of change of yawing-moment coefficient with rolling-angular-velocity factor, which was adverse for the NACA 0012 wing and favorable for the 12-percent-thick biconvex wing.

INTRODUCTION

The advent of the present-day high-speed airplane has caused increased interest in wing sections having sharp leading edges.

Several NACA investigations of the aerodynamic characteristics of such wings have revealed that some of the stability derivatives may be quite different from those of the more conventional wings with round leading edges. For example, the important lateral-control parameter C_{n_p}, the yawing moment due to rolling, has been found to be greatly affected by airfoil section. In the moderate-lift range a sharp-leading-edge airfoil may produce favorable yawing moment due to rolling $\left(\text{positive } C_{n_p}\right)$, whereas the round-nose sections generally cause unfavorable yawing moment due to rolling $\left(\text{negative } C_{n_p}\right)$. This effect of airfoil section was the subject of an investigation made in the Langley free-flight tunnel to determine the dynamic lateral control characteristics of airplane models having wings with either a round-leading-edge airfoil section or a sharp-leading-edge airfoil section.

The two dynamic models used in this investigation had different mass characteristics. One model was representative of a present-day fighter airplane with respect to inertia (normal-inertia model); the other was representative of a possible future type having very high fuselage yawing inertia (high-inertia model). These models were equipped with either of two unswept wings, which were the same except that one was of 12-percent-thick biconvex section which had favorable yawing moment due to rolling and the other was of NACA 0012 section which had adverse yawing moment due to rolling. The directional stability of the models was varied by systematic changes in vertical-tail size.

The investigation consisted of static and rotary force tests made for the purpose of establishing flight conditions, and flight tests from which the dynamic lateral control characteristics of the models with the two wings were evaluated. Some stability parameters affecting the lateral motion of the models were estimated.

SYMBOLS AND COEFFICIENTS

The forces and moments are referred to the stability axes, which are defined as an orthogonal system of axes intersecting at the airplane center of gravity in which the Z-axis is in the plane of symmetry and perpendicular to the relative wind, the X-axis is in the plane of symmetry and perpendicular to the Z-axis, and the Y-axis is perpendicular to the plane of symmetry. A diagram of these axes showing the positive direction of forces and moments is presented in figure 1.

The symbols and coefficients are defined as follows:

C_L lift coefficient (Lift/qS_w)

C_D drag coefficient (Drag/qS_w)

C_m	pitching-moment coefficient $(M/qS_w\bar{c})$
C_Y	lateral-force coefficient (Y/qS_w)
C_l	rolling-moment coefficient (L/qS_wb)
C_n	yawing-moment coefficient (N/qS_wb)
L	rolling moment, about X-axis
M	pitching moment, about Y-axis
N	yawing moment, about Z-axis
Y	lateral force, pounds
q	dynamic pressure, pounds per square foot $\left(\frac{1}{2}\rho V^2\right)$
S_w	wing area, square feet
S_{vt}	vertical tail area, square feet
b	wing span, feet
$\bar{c}$	mean aerodynamic chord, feet $\left(\frac{2}{S_w}\int_0^{b/2} c^2 dy\right)$
c	local wing chord, feet
y	distance along Y-axis
ρ	mass density of air, slugs per cubic foot
V	airspeed, feet per second
β	angle of sideslip, degrees ($-\psi$ in force tests)
ψ	angle of yaw, degrees
Φ	angle of roll, degrees
α	angle of attack, degrees
it	horizontal-tail incidence, degrees
pb/2V	rolling-angular-velocity factor, radians

$rb/2V$ yawing-angular-velocity factor, radians

p rolling angular velocity, radians per second

r yawing angular velocity, radians per second

C_{Y_β} rate of change of lateral-force coefficient with angle of sideslip, per degree $\left(\partial C_Y/\partial\beta\right)$

C_{n_β} directional-stability parameter or rate of change of yawing-moment coefficient with angle of sideslip, per degree $\left(\partial C_n/\partial\beta\right)$

C_{l_β} effective-dihedral parameter or rate of change of rolling-moment coefficient with angle of sideslip, per degree $\left(\partial C_l/\partial\beta\right)$

C_{Y_p} rate of change of lateral-force coefficient with rolling-angular-velocity factor, per radian $\left(\frac{\partial C_Y}{\partial\frac{pb}{2V}}\right)$

C_{n_p} rate of change of yawing-moment coefficient with rolling-angular-velocity factor, per radian $\left(\frac{\partial C_n}{\partial\frac{pb}{2V}}\right)$

C_{l_p} damping-in-roll derivative or rate of change of rolling-moment coefficient with rolling-angular-velocity factor, per radian $\left(\frac{\partial C_l}{\partial\frac{pb}{2V}}\right)$

C_{n_r} damping-in-yaw derivative or rate of change of yawing-moment coefficient with yawing-angular-velocity factor, per radian $\left(\frac{\partial C_n}{\partial\frac{rb}{2V}}\right)$

C_{l_r} rate of change of rolling-moment coefficient with yawing-angular-velocity factor, per radian $\left(\frac{\partial C_l}{\partial\frac{rb}{2V}}\right)$

I_{X_o} moment of inertia about the principal longitudinal axis, slug-feet^2

I_{Y_o} moment of inertia about the principal lateral axis, slug-feet^2

I_{Z_o} moment of inertia about principal normal axis, slug-feet^2

K_{X_o} nondimensional radius of gyration about principal longitudinal axis

K_{Z_o} nondimensional radius of gyration about principal normal axis

K_{XZ} nondimensional product-of-inertia parameter $\left(\left(K_{Z_o}{}^2 - K_{X_o}{}^2\right)\cos \eta \sin \eta\right)$

η angle of attack of principal longitudinal axis of model, positive when principal axis is above flight path at nose, degrees

l longitudinal distance rearward from center of gravity to center of pressure of vertical tail, measured parallel to longitudinal stability axis, feet

z vertical distance upward from center of gravity to center of pressure of vertical tail measured perpendicular to longitudinal stability axis, feet

(Centers of pressure of all vertical tails were assumed to be at 25 percent of the tail mean aerodynamic chord.)

APPARATUS AND MODELS

The flight tests were made in the Langley free-flight tunnel which is described in reference 1. The force tests were made on the free-flight-tunnel six-component balance which is described in reference 2. The rolling derivatives were obtained from the Langley 20-foot free-spinning-tunnel rotary balance which is described in reference 3.

The models consisted of two metal fuselages of different length and mass characteristics upon which were mounted either a 12-percent-thick biconvex section wing with sharp leading edge or an NACA 0012 section wing with round leading edge. The two wings had the same plan forms. Conventional horizontal and vertical stabilizing surfaces were used. The vertical-tail size was varied from 3 to 15 percent of the wing area. The dimensional and mass characteristics of the normal- and high-inertia models are shown in table I and sketches of the models are shown in figure 2. Photographs of the high- and normal-inertia models are presented in figure 3.

DETERMINATION OF STABILITY DERIVATIVES OF FLIGHT-TEST MODELS

The static longitudinal stability characteristics of the complete models were determined from force tests made through an angle-of-attack

range from 0° to 20°. These tests were made at a dynamic pressure of 3.0 pounds per square foot, which corresponds to a test Reynolds number of approximately 350,000, based on the mean aerodynamic chord of 1.38 feet. The results of these tests made to determine the lift, drag, and pitching-moment characteristics of the models equipped with both the biconvex wing and the NACA 0012 wing are shown in figures 4 and 5.

The static-lateral-stability derivatives C_{n_β}, C_{l_β}, and C_{Y_β} presented in table II were determined from measurements of force and moment coefficients at 5° and -5° yaw for the models equipped with the large and small vertical tails and were estimated for the models with intermediate tails. In addition, aileron-effectiveness tests were made for each wing at a dynamic pressure of 3.0 pounds per square foot.

Rotary tests were made to determine the rolling derivatives of each wing alone through an angle-of-attack range from 0° to 14° and of the complete normal-inertia model at 0° and 12° angle of attack. The rotary tests were made at a dynamic pressure of 5.4 pounds per square foot, which corresponds to a test Reynolds number of approximately 590,000, based on the mean aerodynamic chord of 1.38 feet.

The results of rotary tests (C_{n_p}, C_{l_p}, and C_{Y_p}) for the 12-percent-thick biconvex and NACA 0012 wings are shown in figure 6. These data indicate that C_{n_p} is positive for the biconvex section for angles of attack above 6° and negative for the NACA 0012 section throughout the angle-of-attack range up to 13°. The greatest difference between the positive and negative values of C_{n_p} is shown to occur at an angle of attack of about 12°. It was therefore decided to make the flight tests at this angle of attack in order to show the maximum effect of airfoil section.

The data of figure 6 also indicate that the NACA 0012 wing has greater damping in roll than the biconvex wing throughout the angle-of-attack range (C_{l_p} more negative by a constant increment of about 0.06). This difference in the value of C_{l_p} should cause the model with the NACA 0012 wing to roll more slowly than the model with the 12-percent-thick biconvex wing with the same amount of aileron rolling moment. The incremental difference in C_{l_p} throughout the angle-of-attack range for the two wings is not necessarily representative of the effect of airfoil section for all wing plan forms since unpublished results for wings of similar sections but having 45° sweep and taper ratio 1.00 showed that above 7° angle of attack the 12-percent-thick biconvex wing had greater damping in roll than the NACA 0012 wing.

The data of figure 6 also show that C_{Y_p} for the NACA 0012 wing increases more rapidly with angle of attack than for the biconvex wing and has a value about four times as large as that of the biconvex wing

at the angle of attack of the models in the flight tests. This difference in C_{Y_p}, however, is not believed to affect appreciably the lateral controllability of the models.

The wing contributions to the rate of change of yawing-moment coefficient with yawing-angular-velocity factor C_{n_r} and rate of change of rolling-moment coefficient with yawing-angular-velocity factor C_{l_r} were calculated by the methods of references 4 and 5.

In order to determine the total rolling and yawing derivatives for the complete models it was necessary to determine the contribution of the fuselage and vertical tail to each derivative for each flight condition. The fuselage contribution to all derivatives which were estimated was found to be negligible. The vertical-tail contributions to all the rolling and yawing derivatives except C_{n_p} were determined by methods similar to those of references 5 and 6, but since recent NACA tests have indicated a discrepancy between experimental values of $\Delta Cn_{p_{tail}}$ and values calculated by the conventional method of reference 6, estimation of the vertical-tail contribution to the derivative C_{n_p} required special attention. This discrepancy is attributed to wing interference on the flow at the tail surfaces which is not accounted for in the method of reference 6. Inasmuch as the calculated values of $\Delta Cn_{p_{tail}}$ do not include this interference effect and experimental values were deemed necessary, rotary tests of the normal-inertia model were made with the small vertical tails on and off for each of the flight conditions and for the zero angle-of-attack conditions. The experimental values of $\Delta Cn_{p_{tail}}$ as determined from these experiments and the wing-alone experiments are presented in figure 7. The tail contribution to C_{n_p} as calculated by a method similar to that of reference 6 is shown by the solid line in figure 7. The dashed line in figure 7, which represents the calculated values corrected for wing interference, was obtained by drawing a line through the origin parallel to the calculated line. In other investigations this approximate method for correcting for wing interference has been found to give estimated values of $\Delta Cn_{p_{tail}}$ that are in fairly good agreement with experimental data. Inasmuch as this correction method also appears to give fairly good agreement with the limited amount of experimental data obtained from the rotary tests on the present model, it was used to estimate $\Delta Cn_{p_{tail}}$ for the conditions for which force-test data were not obtained.

Values of the various lateral-stability parameters are summarized for each flight condition in table II.

The results of the aileron-effectiveness tests in the form of values of rolling- and yawing-moment coefficients for $\pm 12^{\circ}$ aileron deflection (full control) are as follows:

α (deg)	NACA 0012 wing		12-percent-thick biconvex wing	
	C_l	C_n	C_l	C_n
12	0.031	-0.0050	0.023	-0.0040
14	.028	-.0052	.023	-.0048

The ratio of the aileron rolling moments for the two wings is about the same as the ratio of C_{l_p} for the two wings (fig. 6) for the range of flight conditions (α from 11° to 13°), and thus the aileron effectiveness expressed in terms of the rolling velocity per degree aileron deflection should be the same. Since the yawing moments produced by the ailerons are about equal for the two wings, any appreciable difference in the dynamic lateral control characteristics between the two wings appears to be attributable primarily to the difference in airfoil section.

FLIGHT TESTS

A list of the flight-test conditions is presented in table II. Flight tests of the models were made at angles of attack from 10.8° to 13° which corresponded to a lift-coefficient range of about 0.5 to 0.6. These flight-test conditions were selected so that the maximum effect of airfoil section would be obtained. Flight tests were made with either the NACA 0012 wing or the 12-percent-thick biconvex wing mounted on both the high- and normal-inertia fuselages with vertical tails of various sizes. The models were flown for each test condition with ailerons alone and for some test conditions with combined aileron and rudder control. For flights with combined aileron and rudder, the rudder deflection was adjusted to produce a yawing moment approximately equal and opposite to the adverse yawing moment produced by aileron deflection. Motion-picture records were made to supplement the pilot's observations of each flight condition.

RESULTS AND DISCUSSION

Interpretation of Flight-Test Results

The flight behavior of the model was judged principally on the basis of the amount of adverse yawing motion observed. When ailerons alone were used for control, an adverse yawing motion was readily distinguishable from a favorable yawing motion if the yawing motion was large. When the yawing motion was small, however, it was sometimes difficult to determine whether the yawing motion was favorable or adverse. In these cases the yawing motion with ailerons alone was assumed to be adverse if the yawing motion could be reduced by using the rudder to balance out the adverse yawing moment produced by the ailerons. In flights with combined aileron and rudder control, differences in yawing characteristics of the models with the two wings were attributed to C_{n_p}.

High-Inertia Model

The high-inertia model with the large vertical tail had good flying characteristics with very little yawing motion when equipped with either the NACA 0012 wing or the 12-percent-thick biconvex wing. The yawing behavior of the model with the NACA 0012 wing was considered to be about the same as that of the model with the biconvex wing despite the difference in C_{n_p} (-0.081 for the NACA 0012 model and 0.018 for the biconvex model).

Flight tests of the model with the intermediate tail (conditions II-a and II-b, table II) indicated that with either wing the model was slow to return to zero yaw after being disturbed but still exhibited no evidence of any definite adverse yawing motion. (See fig. 8.)

Flight tests of the model with the NACA 0012 wing and with the small vertical tail installed (condition III, table II) also failed to reveal any definite adverse yawing motion, but the sluggishness in returning from a disturbance in yaw was very pronounced. This sluggishness of the model in returning to zero yaw was attributed to the low values of directional stability $\left(C_{n_\beta} = 0.0003\right)$ and the high inertia in yaw.

Throughout the flight tests of the high-inertia model no definite adverse yawing was observed. This result may be explained as follows: The model rolled much more rapidly than it yawed, partly because of the very small inertia in roll compared with the inertia in yaw $\left(I_{X_O} = 0.167\right.$ slug-ft^2; $\left.I_{Z_O} = 1.616 \text{ slug-ft}^2\right)$ and partly because the aileron rolling moments were much larger than the aileron yawing moments and the yawing moments due to rolling. When the model rolled and yawing moments were

produced, therefore, the time interval before a roll in the opposite direction occurred was so short, because of the inherent rapid rolling response, that the direction of the yawing moment had reversed before any definite yawing motion had a chance to develop.

Normal-Inertia Model

In the flight tests in which the ailerons were used as the sole means of lateral control and the normal-inertia model was equipped with the NACA 0012 wing and small vertical tail (condition IV-a, table II), a relatively large amplitude adverse yawing motion was observed. In this condition the pilot found that the model was difficult to control and that it required a greater amount of aileron control than in previous flights. With the same vertical tail, the model equipped with the 12-percent-thick biconvex wing (condition IV-b, table II) showed little evidence of adverse yawing and was very easy to control. Typical time histories of these two conditions in which the models were controlled by the ailerons alone are presented in figure 9. In the pilot's attempts to maintain straight and level flight, the model equipped with the NACA 0012 wing was found to require more control than the model with the biconvex wing because of its more erratic yawing. This increased control is indicated in figure 9 by the increased length of time the flicker type of control (full on, full off) was held on. A high-amplitude rolling motion resulted for the model equipped with the NACA 0012 wing, and a high-amplitude adverse yawing motion was introduced because of the adverse yawing moments produced by the increased time of aileron deflection and the greater rolling. The flight records of figure 9 indicate that the ratio of yawing to rolling amplitude is approximately 0.8 for the model equipped with the NACA 0012 wing and only about 0.3 for the model with the biconvex wing. This difference in the ratio of yawing to rolling amplitude is attributed directly to the difference in C_{n_p} for the two wings (-0.045 for the NACA 0012 and 0.058 for the biconvex) since the aileron yawing moments are about the same for the two wings.

Flight results for the models controlled by combined ailerons and rudder for the same two conditions (IV-a and IV-b, table II) are presented in figure 10. In these flights, rudder deflection was adjusted to produce a yawing moment approximately equal and opposite to the adverse yawing moment produced by aileron deflection. A comparison between the time histories of figures 9 and 10 indicate that the yawing motion of each model was reduced by the use of rudder control. Since the yawing amplitudes for both models are smaller in figure 10 than in figure 9, the yawing motions of both models appear to be definitely adverse in the flights with ailerons alone.

Figure 10 shows that the model equipped with the biconvex wing had very little yawing motion despite the fact that the favorable yawing moments in this case were greater than the unfavorable yawing moments of the model with the NACA 0012 wing which had a definite adverse yawing motion. This difference in yawing characteristics is attributed, at least in part, to the yawing moments produced by the product of inertia. For a positive value of the product-of-inertia parameter K_{XZ}, a positive rolling acceleration will produce a negative (adverse) yawing moment. Since η, the inclination of the principal longitudinal axis of inertia, was positive for all conditions in the present investigation, the value of K_{XZ} was also positive. It should be expected therefore that rolling accelerations would produce adverse yawing moments that would tend to reinforce the adverse yawing moments produced by C_{n_p} and oppose the favorable yawing moments produced by C_{n_p}.

In an attempt to reduce the effect of adverse C_{n_p} on the flight characteristics of the model with the NACA 0012 wing, flights with ailerons alone were made with a series of larger vertical tails to increase the directional stability and damping in yaw until the flight characteristics were as good as those of the model with the biconvex wing and the small vertical tail (condition IV-b, table II). As flights were made with progressively larger vertical tails, a reduction in the amount of adverse yawing motion was noted. It was necessary, however, to use a vertical tail over four times as large as that of condition IV-b in order to obtain comparable flight characteristics for the NACA 0012 wing. A time history of a flight of the model with the large vertical tail (condition V) is shown in figure 11. A comparison of this time history with that of the biconvex model in figure 9 (condition IV-b) shows that the amplitudes of the rolling and yawing motions for the two conditions are similar. The favorable effect of the large increase in C_{n_β} (0.0010 to 0.0035) caused by increasing the vertical-tail area was probably partly offset by the unfavorable effect of the increase in adverse C_{n_p} (-0.045 to -0.062). (See table II.)

CONCLUDING REMARKS

A flight investigation in the Langley free-flight tunnel of models equipped with NACA 0012 (round-leading-edge) and 12-percent-thick biconvex (sharp-leading-edge) wings indicated that, for the conditions of the tests, no apparent effect of airfoil section on the flying characteristics of a model having high inertia in yaw was noted, even at low values of directional stability. For the flight conditions investigated the normal-inertia model equipped with the NACA 0012 wing revealed an adverse yawing motion which increased with reduced values of directional stability, but when the

model was equipped with the 12-percent-thick biconvex wing practically no adverse yawing was observed, even at the lowest values of directional stability.

Langley Aeronautical Laboratory
National Advisory Committee for Aeronautics
Langley Air Force Base, Va., September 5, 1950

REFERENCES

1. Shortal, Joseph A., and Osterhout, Clayton J.: Preliminary Stability and Control Tests in the NACA Free-Flight Wind Tunnel and Correlation with Full-Scale Flight Tests. NACA TN 810, 1941.

2. Shortal, Joseph A., and Draper, John W.: Free-Flight-Tunnel Investigation of the Effect of the Fuselage Length and the Aspect Ratio and Size of the Vertical Tail on Lateral Stability and Control. NACA ARR 3D17, 1943.

3. Stone, Ralph W., Jr., Burk, Sanger M., Jr., and Bihrle, William, Jr.: The Aerodynamic Forces and Moments on a $\frac{1}{10}$-Scale Model of a Fighter Airplane in Spinning Attitudes as Measured on a Rotary Balance in the Langley 20-Foot Free-Spinning Tunnel. NACA TN 2181, 1950.

4. Toll, Thomas A., and Queijo, M. J.: Approximate Relations and Charts for Low-Speed Stability Derivatives of Swept Wings. NACA TN 1581, 1948.

5. Campbell, John P., and Goodman, Alex: A Semiempirical Method for Estimating the Rolling Moment Due to Yawing of Airplanes. NACA TN 1984, 1949.

6. Bamber, Millard J.: Effect of Some Present-Day Airplane Design Trends on Requirements for Lateral Stability. NACA TN 814, 1941.

TABLE I.- DIMENSIONAL AND MASS CHARACTERISTICS OF MODELS

	High inertia	Normal inertia
Weight, lb	17.8	14.4
Moments of inertia:		
I_{X_o}, slug-ft^2	0.167	0.199
I_{Y_o}, slug-ft^2	1.371	0.355
I_{Z_o}, slug-ft^2	1.616	0.551
Radii of gyration:		
K_{X_o}	0.138	0.142
K_{Z_o}	0.429	0.278
Product of inertia:		
K_{XZ}	0.0075	0.0162
η, deg	7.5	10.2
Wing:		
Area, sq ft	5.33	5.33
Span, ft	4.00	4.00
Aspect ratio	3.00	3.00
Taper ratio	0.50	0.50
$\bar{c}$, ft	1.38	1.38
Root chord, ft	1.78	1.78
Tip chord, ft	0.89	0.89
Loading, lb/sq ft	3.34	2.70
Airfoil sections	NACA 0012 12-percent-thick biconvex	NACA 0012 12-percent-thick biconvex
Tail length:		
l/b at $\alpha = 0^\circ$ (with small vertical tails)	0.740	0.477

NACA

TABLE II

AERODYNAMIC PARAMETERS OF COMPLETE MODELS

Flight condition	Fuselage	Wing section	Tail (S_{vt}/S_w)	C_{n_p} (per radian) (a)	C_{l_p} (per radian) (a)	C_{Y_p} (per radian) (a)	C_{n_r} (per radian) (a,b)	C_{l_r} (per radian) (c)	C_{n_β} (per deg)	C_{l_β} (per deg)	C_{Y_β} (per deg)	C_L	α (deg)
I-a	High inertia	NACA 0012	Large (0.13)	-0.081	-0.31	0.103	-0.207	[d]0.178	0.0023	-0.0007	-0.0070	0.62	12.0
I-b	----do-----	12-percent-thick biconvex	----do------	.018	-.22	.029	-.205	[d].151	.0023	-.0011	-.0072	.57	12.5
II-a	----do-----	NACA 0012	Intermediate (0.06)	-.058	-.31	.110	-.143	[a].197	[e].0013	[e]-.0008	[e]-.0060	.65	12.4
II-b	----do-----	12-percent-thick biconvex	----do-----	.041	-.22	.038	-.140	[a].182	[e].0013	[e]-.0014	[e]-.0060	.57	12.5
III	----do-----	NACA 0012	Small (0.03)	-.045	-.32	.101	-.069	[d].207	.0003	-.0012	-.0047	.60	11.5
IV-a	Normal inertia	NACA 0012	----do-----	-.045	-.32	.097	-.052	[d].180	.0010	-.0008	-.0025	.48	11.0
IV-b	-----do-------	12-percent-thick biconvex	----do----	.058	-.20	.019	-.052	[d].176	.0008	-.0013	-.0027	.46	13.0
V	-----do-------	NACA 0012	Extra large (0.15)	-.062	-.32	.058	-.160	[d].160	.0035	-.0011	-.0075	.47	10.8

[a]Tail contributions were determined from the following equations:

$$\Delta C_{n_{p_{tail}}} = -2(57.3)\left(\frac{l}{b}\right)\left(\frac{z}{b}\right)\Delta C_{Y_{\beta_{tail}}} + \text{Wing interference effect}$$

$$\Delta C_{l_{p_{tail}}} = 2(57.3)\left(\frac{z}{b}\right)^2 \Delta C_{Y_{\beta_{tail}}}$$

$$\Delta C_{Y_{p_{tail}}} = 2(57.3)\left(\frac{z}{b}\right)\Delta C_{Y_{\beta_{tail}}}$$

$$\Delta C_{n_{r_{tail}}} = 2(57.3)\left(\frac{l}{b}\right)^2 \Delta C_{Y_{\beta_{tail}}}$$

$$\Delta C_{l_{r_{tail}}} = -2(57.3)\left(\frac{l}{b}\right)\left(\frac{z}{b}\right)\Delta C_{Y_{\beta_{tail}}}$$

[b]Wing contribution by method of reference 4.
[c]Wing contribution by method of reference 5.
[d]Tail contribution by method of reference 5.
[e]Estimated value.

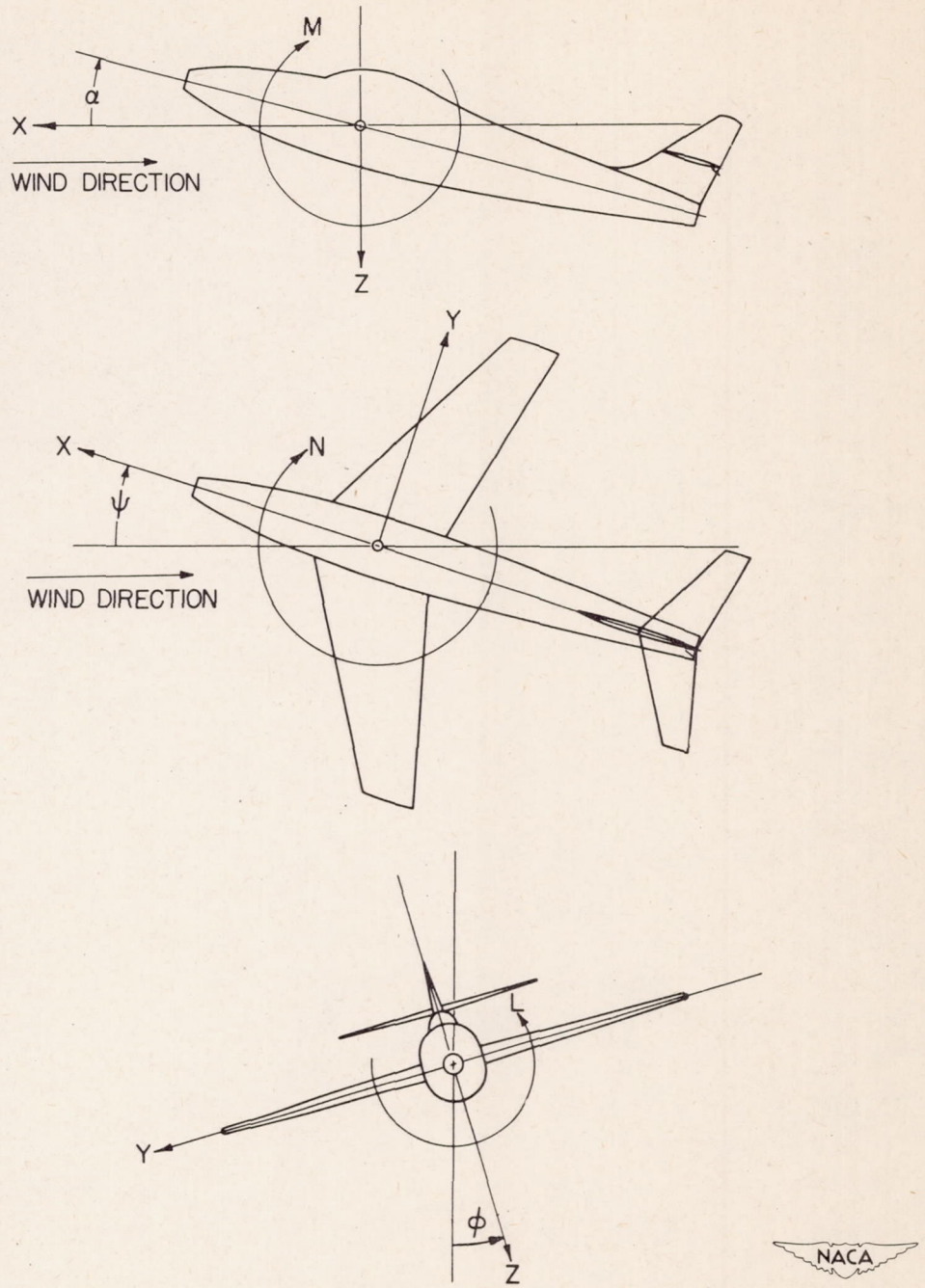

Figure 1.- The stability system of axes. Arrows indicate positive directions of moments, forces, and angles.

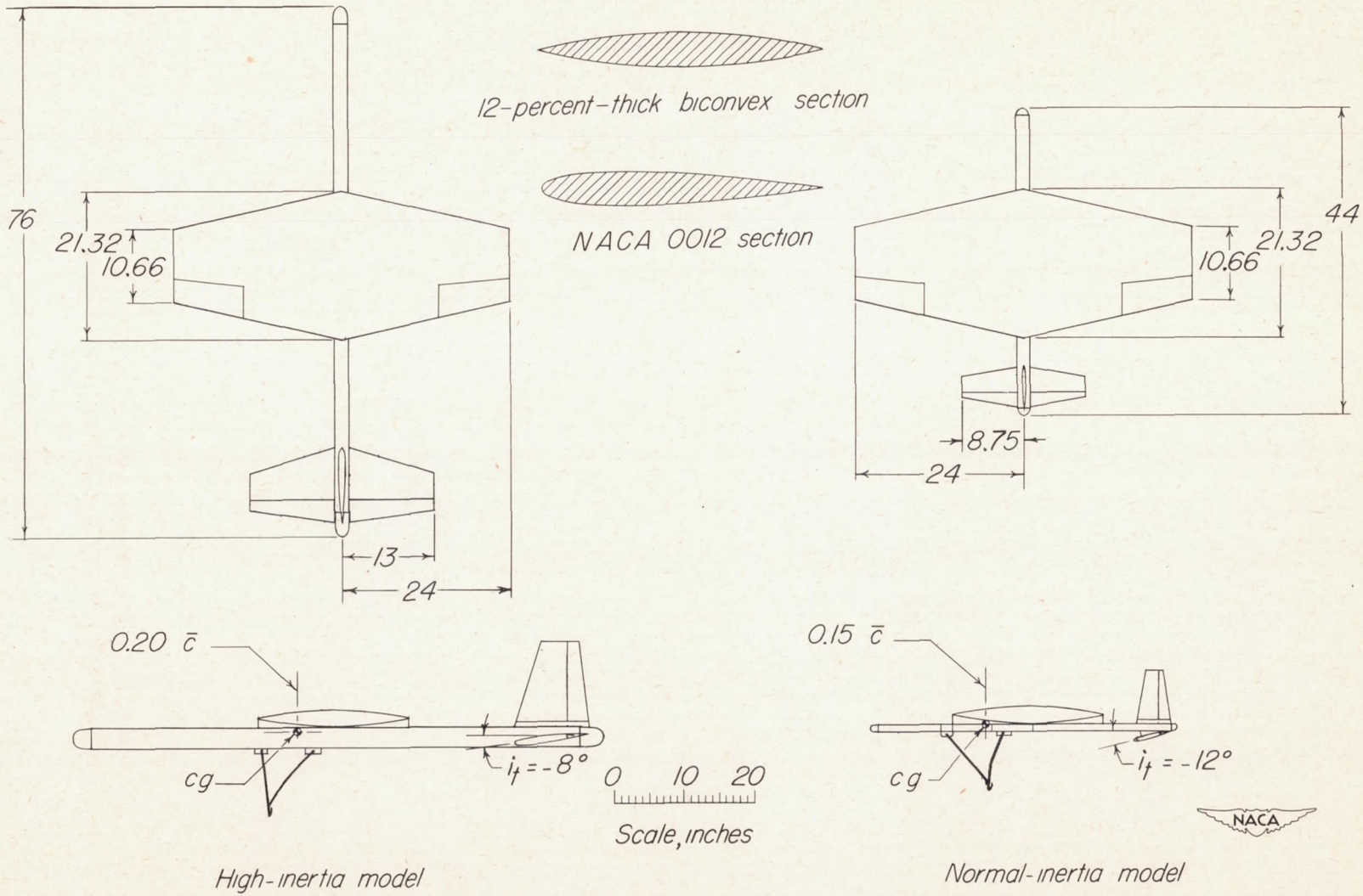

Figure 2.- Two-view sketches of the high- and normal-inertia models. Tail incidence values shown are for the flight conditions.

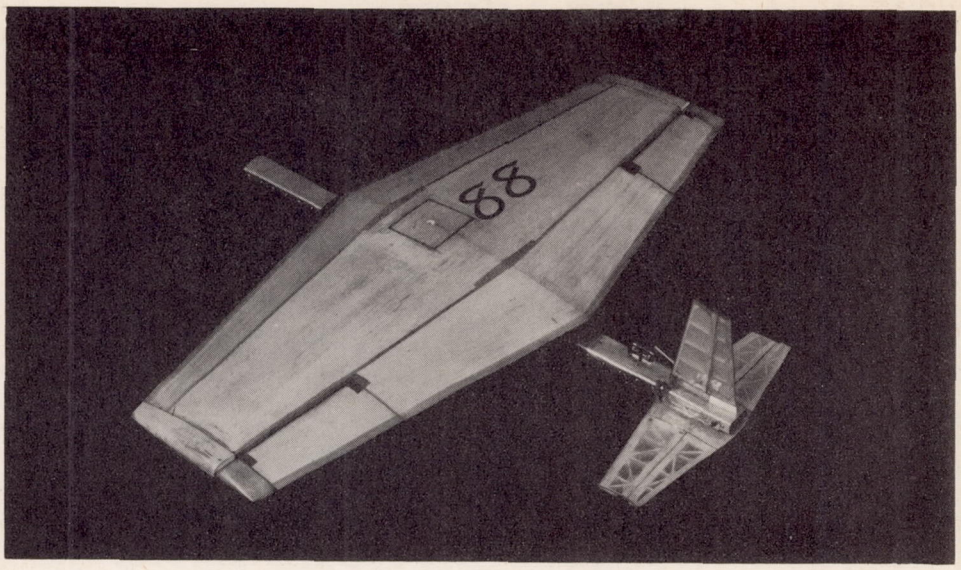

(a) Normal-inertia model.

NACA
L-66732

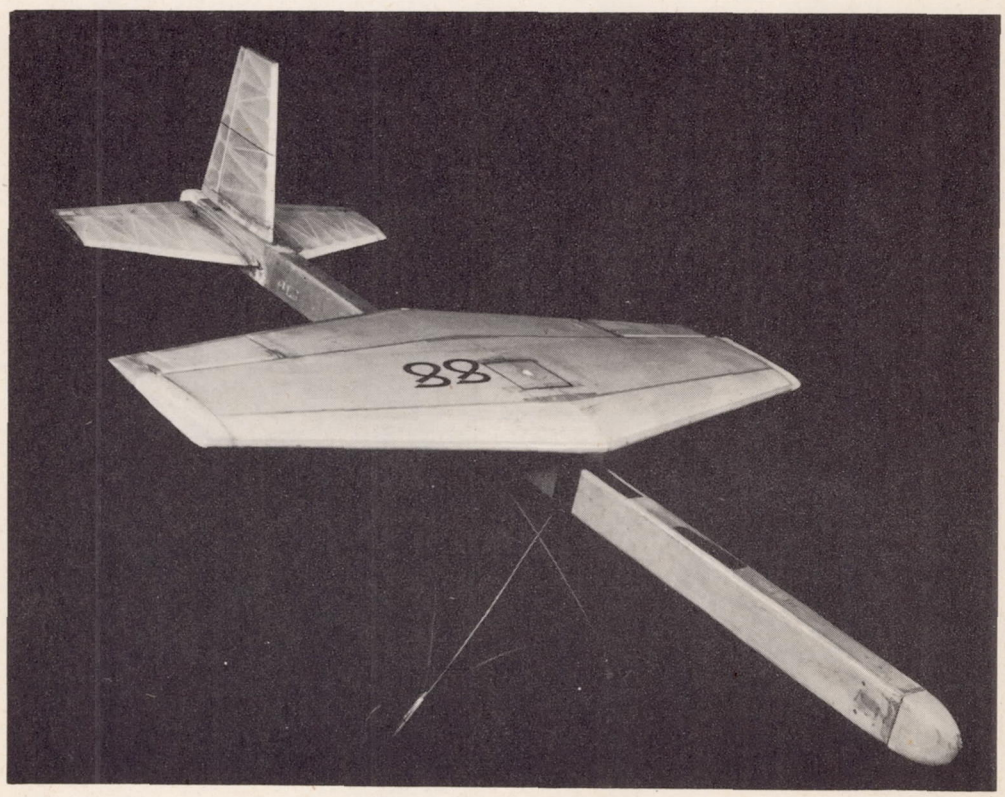

(b) High-inertia model.

NACA
L-66737

Figure 3.- Normal- and high-inertia models.

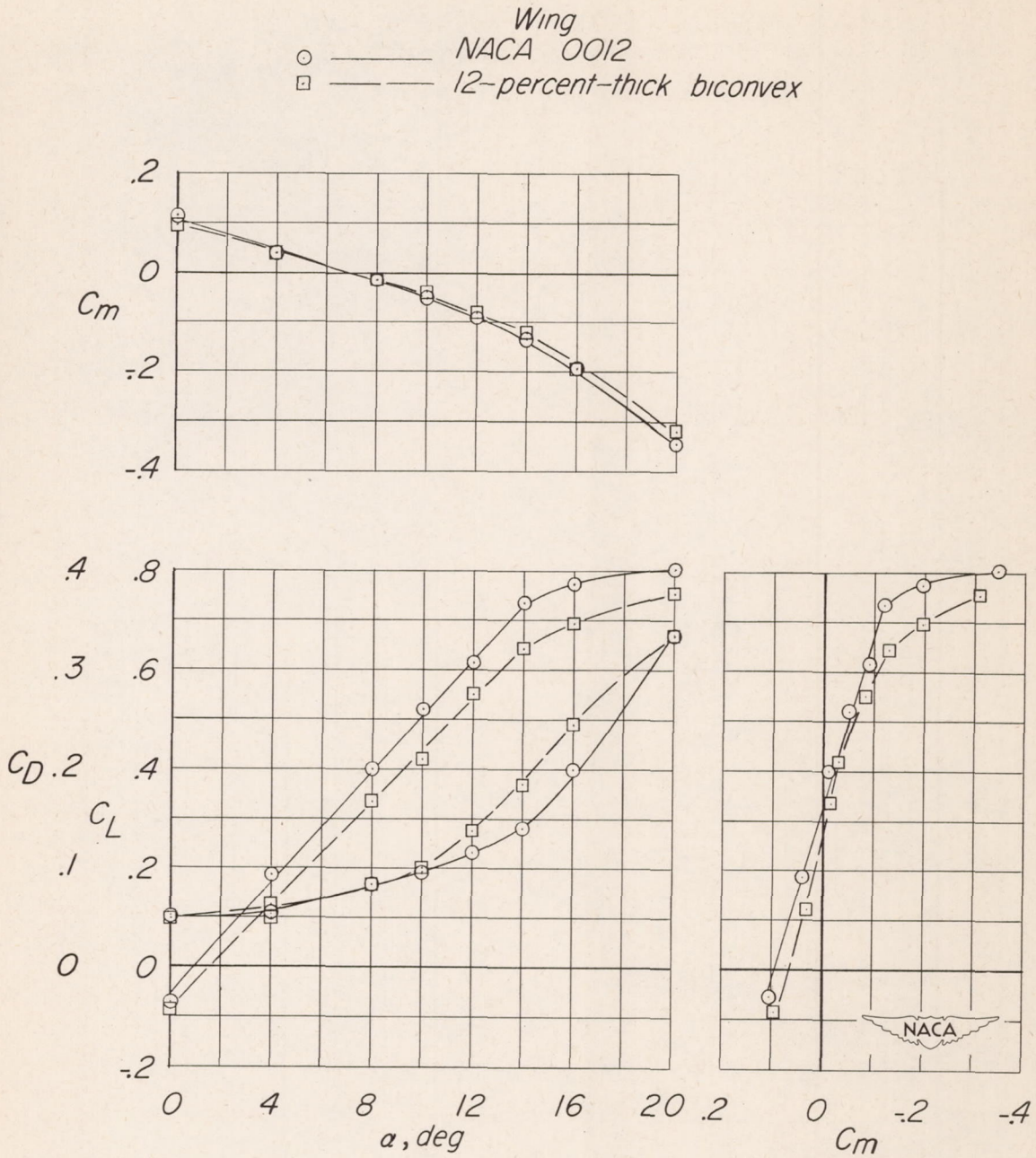

Figure 4.- Lift, drag, and pitching-moment characteristics of the high-inertia model equipped with the NACA 0012 and 12-percent-thick biconvex wings. Center of gravity at $0.20\bar{c}$; $i_t = -6^\circ$.

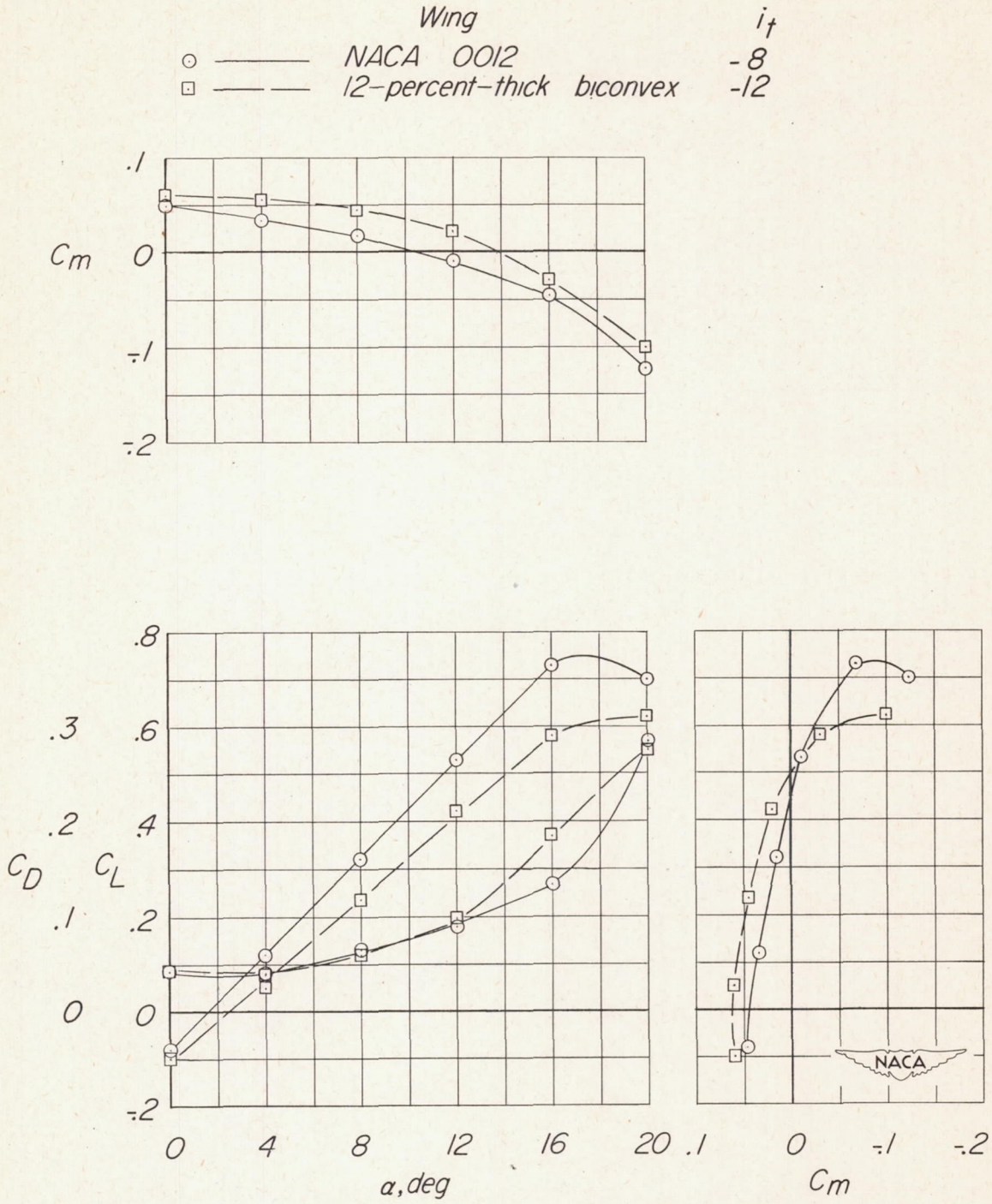

Figure 5.- Lift, drag, and pitching-moment characteristics of the normal-inertia model equipped with the NACA 0012 and 12-percent-thick biconvex wings. Center of gravity at 0.15$\bar{c}$.

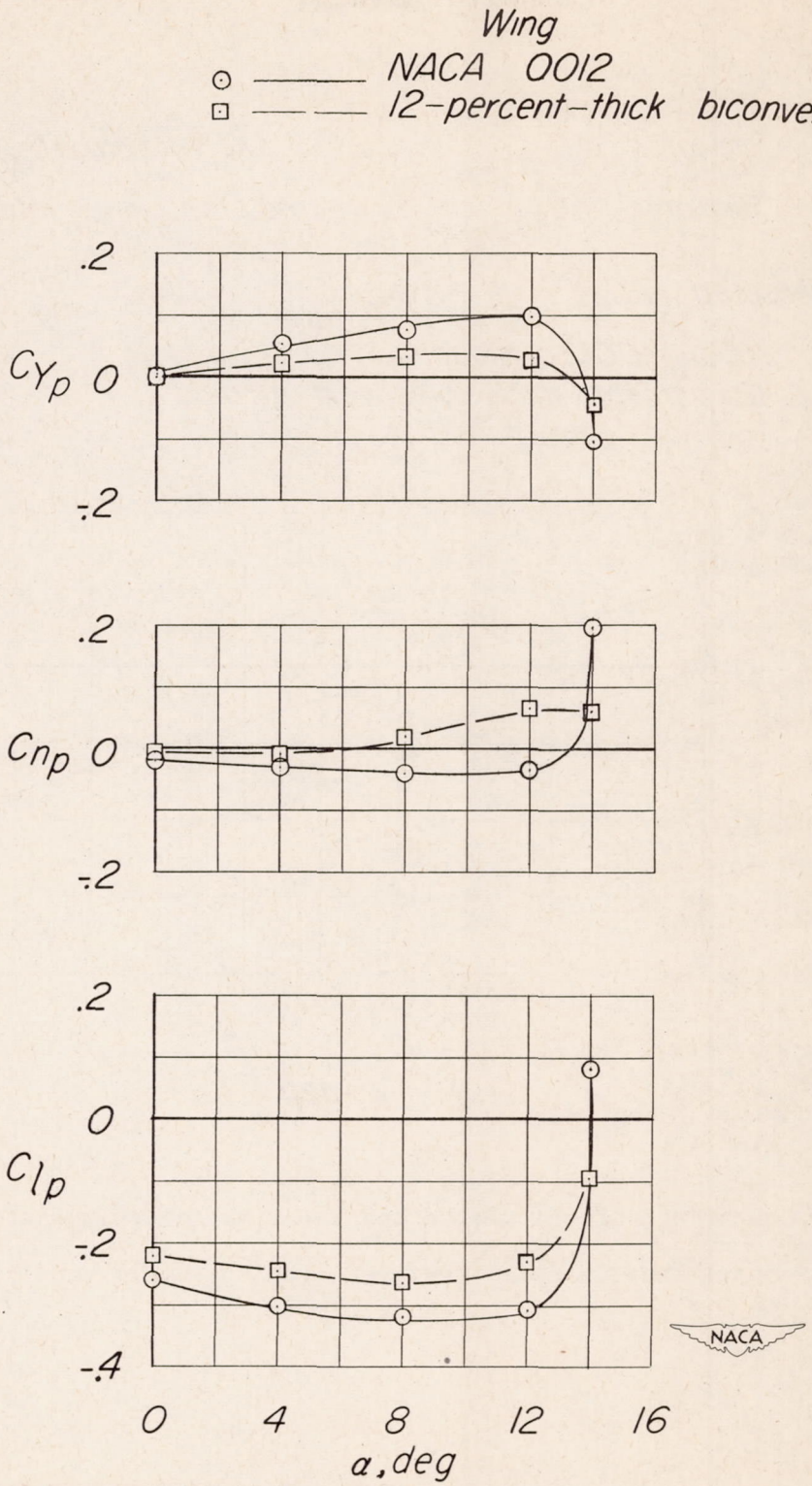

Figure 6.- Variation of the rolling derivatives with angle of attack for the NACA 0012 and 12-percent-thick biconvex wings alone.

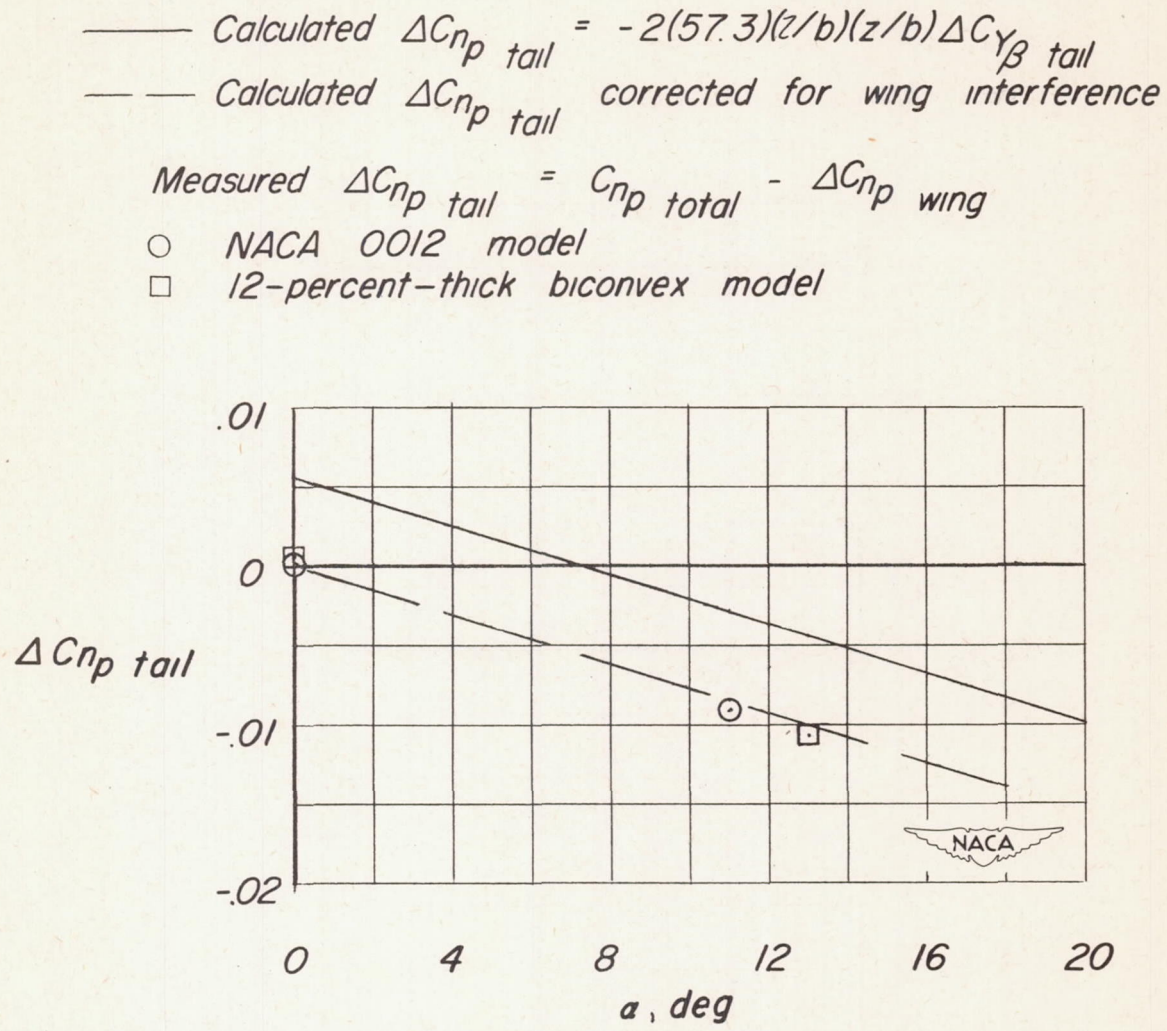

Figure 7.- Comparison of calculated and experimental values of $\Delta C_{n_{p_{tail}}}$ for the normal-inertia model equipped with the small vertical tail.

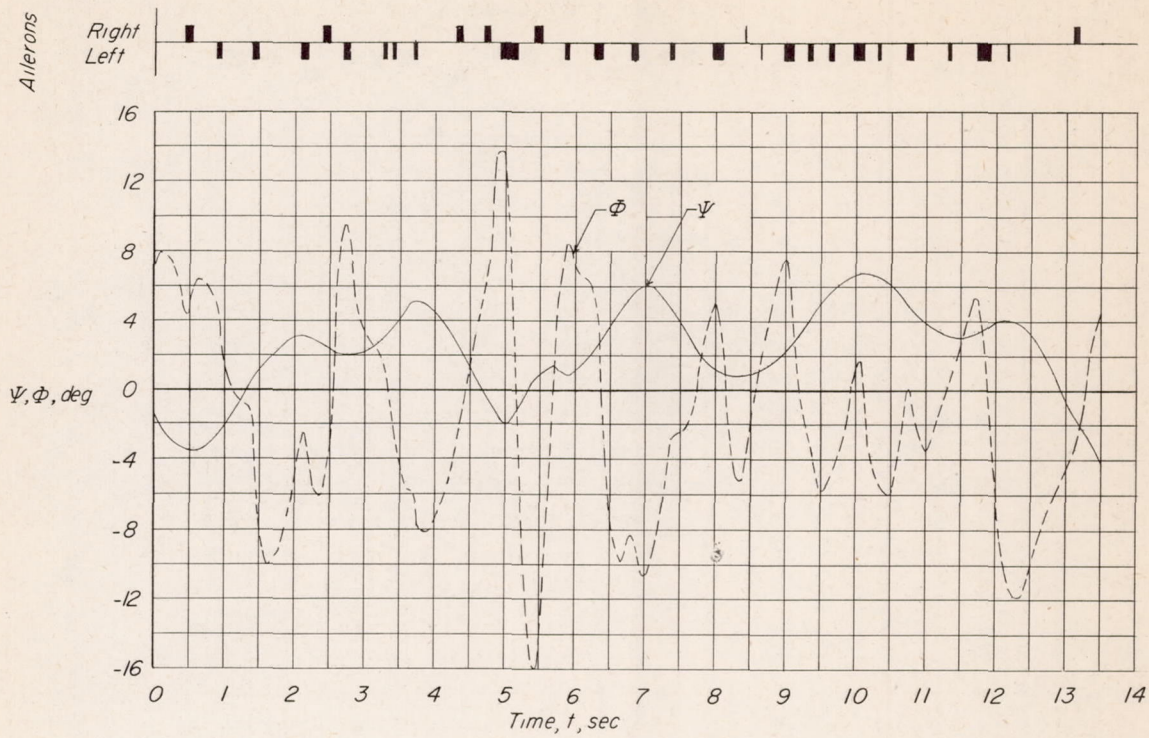

(a) Condition II-a. NACA 0012 wing; $C_{n_p} = -0.058$.

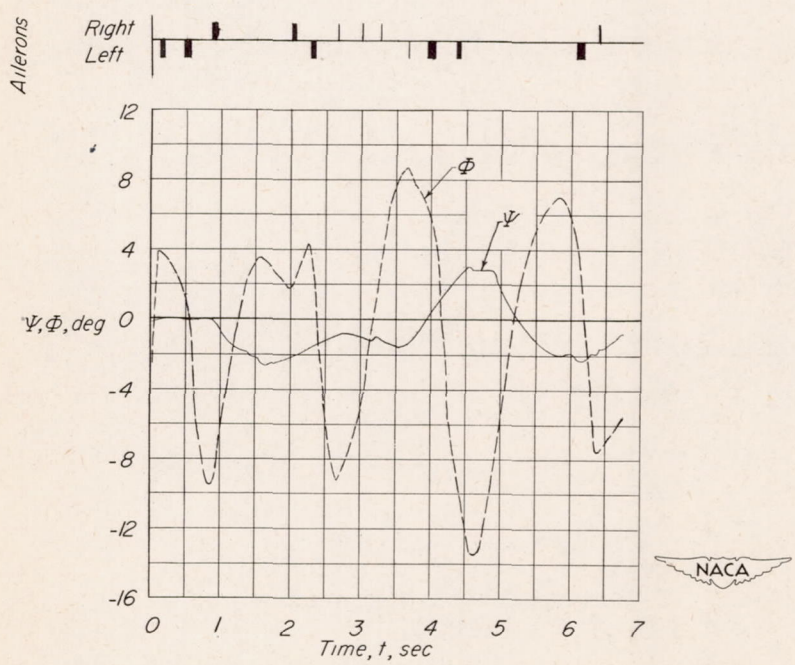

(b) Condition II-b. 12-percent-thick biconvex wing; $C_{n_p} = 0.041$.

Figure 8.- Time histories of flights of the high-inertia model controlled by ailerons alone. $C_{n_\beta} = 0.0013$; $KX_o = 0.138$; $KZ_o = 0.429$.

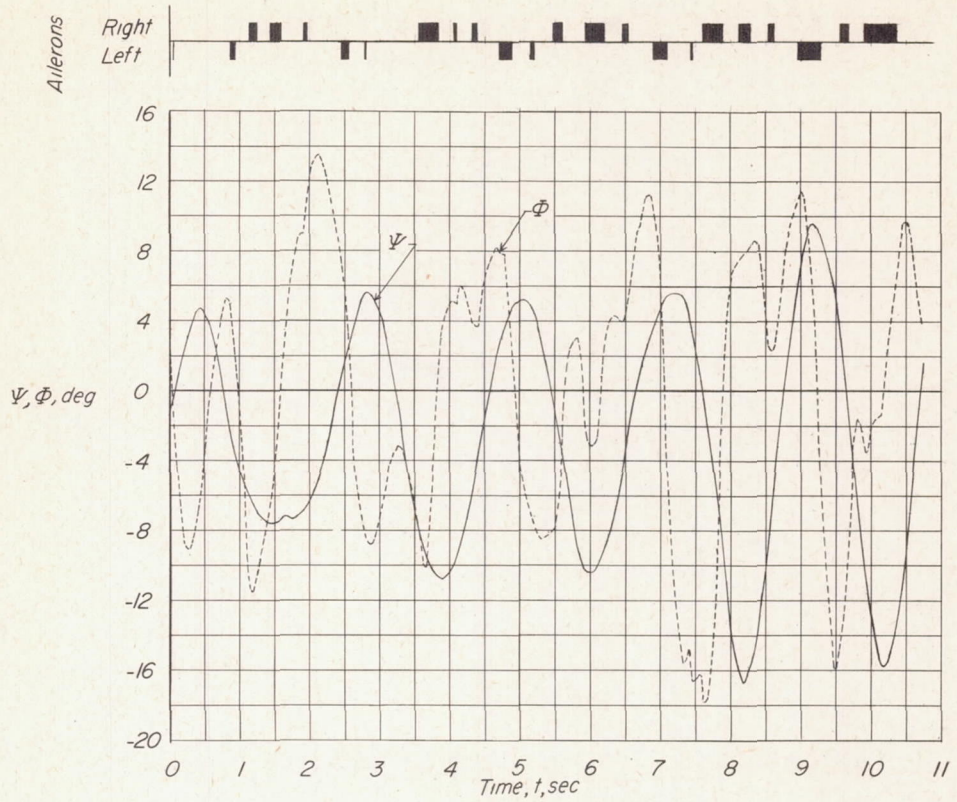

(a) Condition IV-a. NACA 0012 wing; $C_{n_p} = -0.045$; $C_{n_\beta} = 0.0010$.

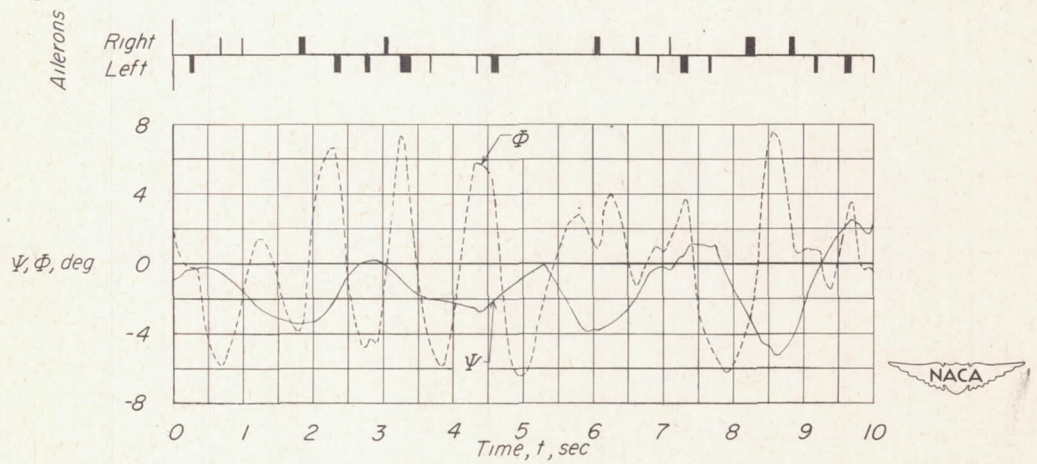

(b) Condition IV-b. 12-percent-thick biconvex wing; $C_{n_p} = 0.058$; $C_{n_\beta} = 0.0008$.

Figure 9.- Time histories of flights of the normal-inertia model controlled by ailerons alone. $K_{X_o} = 0.142$; $K_{Z_o} = 0.278$.

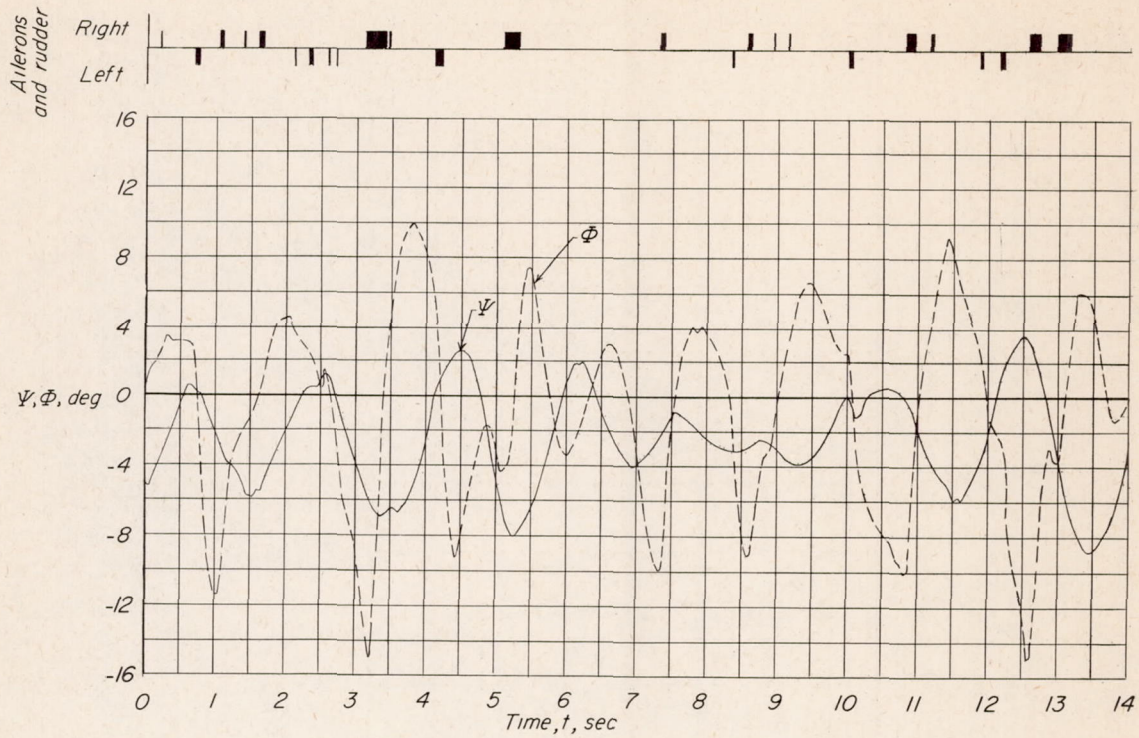

(a) Condition IV-a. NACA 0012 wing; C_{n_p} = -0.045; C_{n_β} = 0.0010.

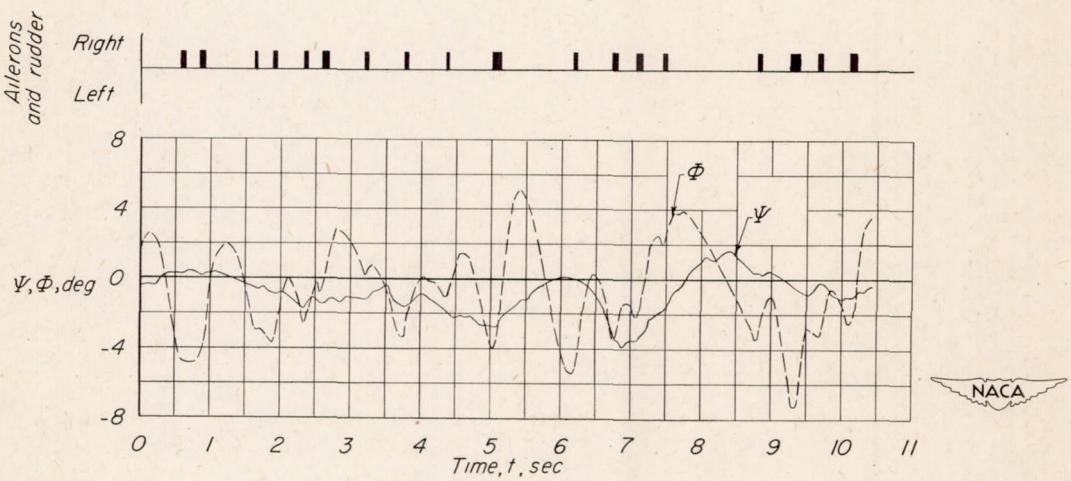

(b) Condition IV-b. 12-percent-thick biconvex wing; C_{n_p} = 0.058; C_{n_β} = 0.0008.

Figure 10.- Time-histories of flights of the normal-inertia model controlled by ailerons and rudder. K_{X_o} = 0.142; K_{Z_o} = 0.278.

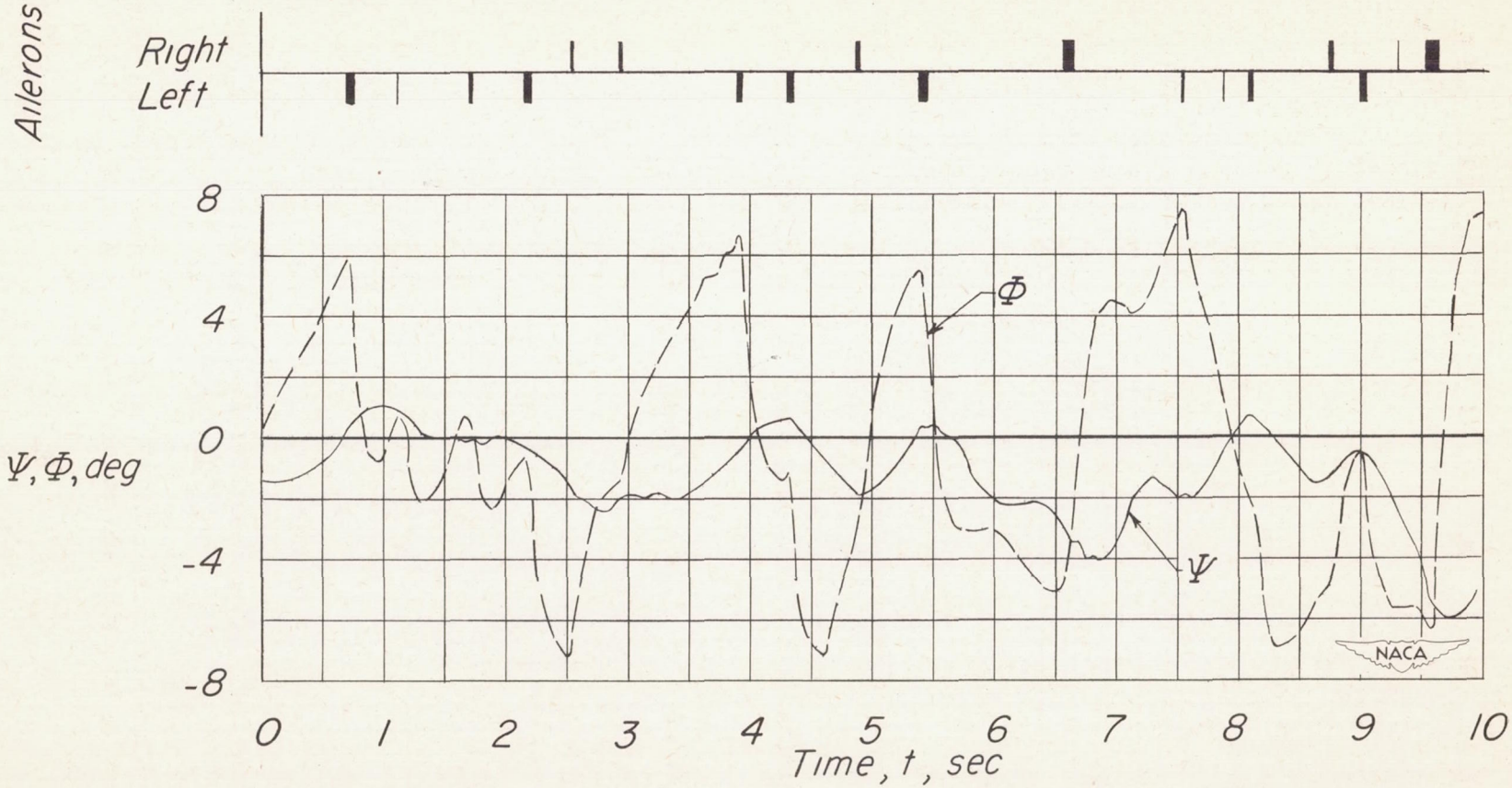

Figure 11.- Time history of a flight of the normal-inertia model equipped with the NACA 0012 wing and the extra large vertical tail. Control by ailerons alone. $K_{X_o} = 0.167$; $K_{Z_o} = 0.280$; $C_{n_\beta} = 0.0035$; $C_{n_p} = -0.062$.

NACA-Langley - 11-10-50 - 1000